Journal of Alloys and Compounds 513 (2012) 184–188

Contents lists available at SciVerse ScienceDirect

Journal of Alloys and Compounds

journal homepage: www.elsevier.com/locate/jallcom

Visible light induced electron transfer behavior of a CeO_2-loaded HfO_2/carbon cluster nanocomposite material

H. Matsui [a], M. Nishii [a], S. Karuppuchamy [b,*], J.-M. Jeong [c], M.A. Hassan [b], M. Yoshihara [a]

[a] Department of Applied Chemistry, Faculty of Science and Engineering, Kinki University, 3-4-1 Kowakae, Higashiosaka, Osaka 577-8502, Japan
[b] Institute of Bioscience, Universiti Putra Malaysia, 43400 Serdang, Selangor, Malaysia
[c] Research and Development Centre, TSM Co. Ltd., Eoro-ri 625, Buksan-eup, Chilgok-kun, Gyeongsangbuk-do 718-844, South Korea

ARTICLE INFO

Article history:
Received 6 April 2011
Received in revised form 4 October 2011
Accepted 6 October 2011
Available online 18 October 2011

Keywords:
Semiconductors
Polymers
Nanostructures
Inorganic compounds
Electronic structure

ABSTRACT

The microwave-irradiated calcination of $HfOCl_2$/starch complex I under an air atmosphere produced the HfO_2/carbon cluster composite material which is denoted as Ic. The obtained composite material could decompose methylene blue under the irradiation of light ($\lambda > 460$ nm). The surface of Ic was loaded with CeO_2 particles to obtain CeO_2-loaded composite material, which can decompose the aqueous silver nitrate solution and produce O_2 and Ag in the ratio of 1:4.2. Water photo-decomposition experiment was also carried out using Pt-modified composite materials.

1. Introduction

Multi-electron transport by photo-irradiation has attracted attention among the scientists, because such a transport could play a key role to achieve functional materials such as molecular electronic devices [1], photocatalysts [2–7], and solar cells [8–10]. Wide band gap oxide semiconductors have been the most widely researched photocatalysts, but suffer from low efficiency and narrow light response range. Combining semiconductors with carbonaceous nanomaterials is being increasingly investigated as a means to increase photocatalytic activity, and demonstrations of enhancement are quite plentiful [11–15]. The carbonaceous material modified semiconductors are obtained by using various form of carbon such as activated carbon [16–19], carbon nanotubes [20], fullerenes [21], graphene [22–24] and nanometric carbon black [25–27]. We are also currently witnessing widespread academic and technological interest in the relatively new field of carbonaceous semiconductor hybrid materials. Of such materials, carbon cluster-sensitized inorganic semiconductors (composite materials) which are used in photocatalysts are particularly appealing to us and we have a few specific contributions relevant to this field [28–33]. In particular, we have reported a novel and relatively simple technique to synthesize a composite material by the calcination of either metal-organic moiety hybrid copolymers or inorganic metal compound/organic polymer complexes [28–33]. Indeed, we have observed the electron transfer feature of carbon cluster → HfO_2 in HfO_2/carbon cluster composite material and CeO_2 → carbon cluster in CeO_2/carbon cluster composite material. In this work, we report the synthesis, structural characterizations and electronic behaviors of HfO_2/carbon cluster composite material Ic and CeO_2-loaded HfO_2/carbon cluster composite material Ic·CeO_2 (Scheme 1).

2. Experimental

2.1. Reagents

$HfOCl_2 \cdot 8H_2O$, tris(acetylacetonato)cerium(III) trihydrate $Ce(acac)_3$, starch, hydrogen hexachloroplatinate hexahydrate, 1,1-diphenyl-2-picrylhydrazyl (DPPH), methylene blue, citric acid, and silver nitrate ($AgNO_3$) were used as received. All of the chemicals were purchased from Wako Pure Chemicals, Japan.

2.2. Synthesis of precursor I

A mixture of 7.09 g (17.29 mmol) of $HfOCl_2 \cdot 8H_2O$ and 22.89 g (141.3 mmol) of starch in 100 mL of distilled water was stirred at room temperature for 1 h. After water was evaporated under a reduced pressure, the solids were dried at 60 °C under a vacuum condition for overnight to obtain precursor I.

2.3. Calcination of precursor I

4 g of Precursor I was put into in the porcelain crucible and then it was covered with alumina–silica wool and finally it was treated by microwave irradiation using

* Corresponding author. Tel.: +60 38946 7593.
E-mail addresses: skchamy@gmail.com, skchamy@ibs.upm.edu.my (S. Karuppuchamy).

0925-8388/$ – see front matter © 2011 Elsevier B.V. All rights reserved.
doi:10.1016/j.jallcom.2011.10.016

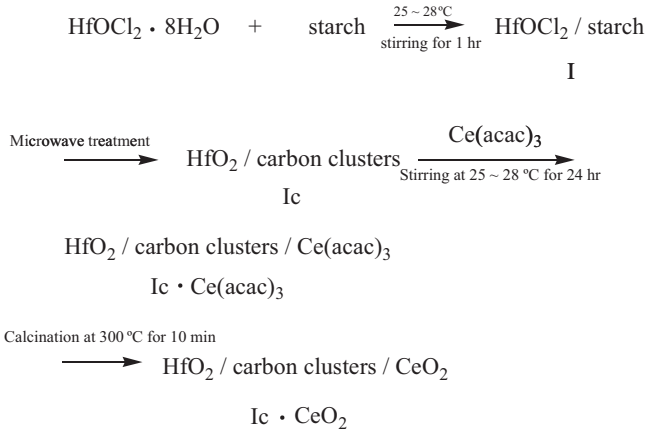

Scheme 1. Synthesis of materials.

LG Company MJ-60HL5 (2450 MHz, 500 W) for 3, 6 and 9 min to obtain calcined materials Ic-3, Ic-6 and Ic-9, respectively.

2.4. CeO_2-loading on the surface of Ic-6

A mixture of 300 mg of Ic-6 and 52.61 mg (0.375 mmol) of $Ce(acac)_3$ in 60 mL of THF was stirred at room temperature for 24 h. The precipitate was collected and dried at 60 °C under a vacuum to obtain $Ce(acac)_3$-loaded material Ic-6·$Ce(acac)_3$. Then the complex was heated at 300 °C for 10 min under an air atmosphere using Barnstead Thermolyne electric furnace FB1300 to obtain CeO_2-loaded HfO_2/carbon cluster composite material Ic-6·CeO_2.

2.5. Surface modification of Ic-6·CeO_2 and Ic-6 with Pt particles

A mixture of 30 mg of Ic-6·CeO_2 and 0.8 mL of methanol was added into 0.8 mL of an aqueous 0.05 mmol/L hydrogen hexachloroplatinate(IV) solution, and then the mixture was stirred at room temperature under the irradiation of light above 460 nm for 30 min using Hoya–Schott Megalight halogen lamp (100 W). The precipitate was collected, washed with distilled water and dried at 60 °C under a reduced pressure for overnight to obtain Pt-modified material Ic-6·CeO_2·Pt. Similar treatment of Ic-6 produced the corresponding Pt-modified material Ic-6·Pt.

2.6. Characterization

Elemental analysis was performed for C and H using Yanaco MT-6, for Cl using Yanaco YS-10, and for Hf, Ce and Pt by inductively coupled plasma atomic emission spectrometry (ICP-AES) using Shimadzu ICP-7500. Raman spectrum was measured on a single-grating spectrometer (Jobin Yvon HR-800) equipped with an Ar ion laser at 514.5 nm for the excitation. Scanning electron microscope coupled with energy dispersive X-ray spectroscopy (SEM–EDX) measurement was carried out using Hitachi High technologies S-4800 FE-SEM and Horiba Emax Energy EX-450. X-ray diffraction (XRD) spectra were taken using Rigaku Mini Flex. X-ray photospectrometry (XPS) spectra were measured using Shimadzu ESCA-850. Transmission electron microscopy (TEM) observations were done using Jeol JEM-3010. Electron spin resonance (ESR) spectra were measured using Jeol JES-TE200. UV–vis spectra were taken using Hitachi U-4000 spectrometer. Visible light was generated using Hoya–Schott Megalight 100 halogen lamp. TCD gas chromatogram was taken using Shimadzu GC-8A gas chromatography.

The reduction reaction of methylene blue in the presence of calcined material Ics was carried out as follows. A mixture of 3 mg of Ics and 10 mL of 0.03 mmol methylene blue and 0.12 mmol citric acid aqueous solution was stirred at room temperature in the dark for overnight. The citric acid was used as electron donor reagent. The mixture was irradiated by visible light (light intensity = 2 mW/cm^2) above the wavelength of 460 nm under an argon atmosphere and the concentration of methylene blue was estimated by UV–vis spectral analysis.

The oxidation–reduction reaction of an aqueous silver nitrate solution in the presence of Ic-6·CeO_2 was performed in the following way. 10 mg of Ic-6·CeO_2 was added to 1 mL of an aqueous 0.05 mol/L silver nitrate solution and then it was deaerated by argon bubbling for 1 h and finally the mixture was irradiated by visible light above 460 nm. The evolved O_2 gas was estimated by gas chromatography and the obtained Ag was analyzed by ICP.

Water photo-decomposition experiment in the presence of Ic-6·CeO_2·Pt, Ic-6·CeO_2, Ic-6·Pt and Ic-6 was performed and details are given below. 10 mg of the material was added into 0.2 mL of distilled water and then deaerated by argon bubbling for 1 h in the dark. Visible light ($\lambda > 460$ nm) was irradiated to the mixture for 3 h, and the evolved H_2 and O_2 gases were estimated by gas chromatography.

Table 1
Elemental analysis of precursor I and calcined materials Ics.

Materials	Found (%)			
	Hf	C	H	Cl
I	9.86	32.59	5.34	3.07
Ic-3	30.86	55.27	2.10	0
Ic-6	30.01	55.41	1.62	0
Ic-9	33.36	57.99	0.32	0

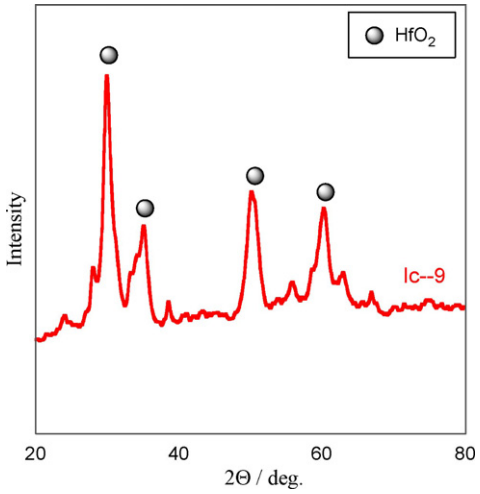

Fig. 1. XRD pattern of calcined material Ic-9.

3. Results and discussion

The elemental analysis of precursor I (Table 1) shows the presence of Hf and Cl atoms. The SEM–EDX spectra of precursor I reveals that the Hf atom is homogeneously dispersed in the matrix. The above results clearly indicate the formation of precursor I. The microwave-irradiated calcination of I produced black-colored materials Ics. The results of the elemental analysis of Ics are also shown in Table 1. The content of H decreases with the increase of irradiation time, indicating that the carbonization of the material was successfully carried out. The XRD patterns of Ic-9 (Fig. 1) show main peaks at $2\theta = 28.4°$, 35.2°, 50.2°and 60.1° due to HfO_2. The XPS analysis of Ics show binding energies at 214.0–214.1 eV due to the Hf_{4d} orbital of HfO_2. The TEM observations of samples Ic-3, Ic-6 and Ic-9 showed particles with the diameters of ca. 10, 20 and 50 nm, possibly HfO_2, in the carbon phases. These results indicated that the calcined materials are composed of nano-sized HfO_2 and carbon cluster.

The electronic behavior of the calcined materials was also examined. The ESR spectra of Ics (Fig. 2) show a peak at 337 mT ($g = 2.003$). The radical spin quantity (*rsq*) of the calcined materials was determined by the double integrating calculation of the differential absorption line with the use of DPPH (Table 2), and the highest *rsq* value was obtained for Ic-6. It is assumed that an electron transfer between the HfO_2 particle and the carbon cluster takes place to form a free electron on the carbon cluster and therefore the highest charge separation occurred for Ic-6. The largest *rsq* value of Ic-6, indicates that the most effective charge separation can takes place

Table 2
Radical spin quantity (*rsq*) and reduction activity (*ra*) of calcined materials Ics.

Materials	*rsq* (spins/g)	*ra* (μmol/g h)
Ic-3	2.97×10^{19}	2.18
Ic-6	1.55×10^{20}	2.58
Ic-9	5.76×10^{19}	0.63

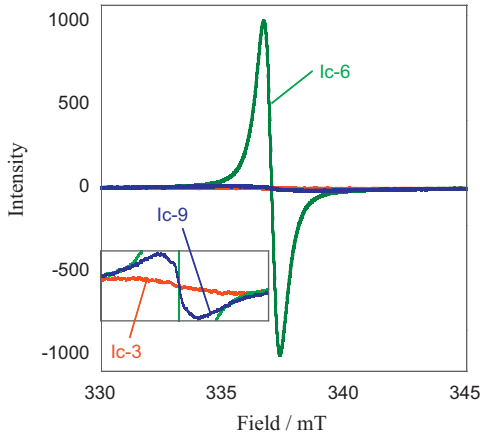

Fig. 2. ESR spectra of calcined materials Ics.

in Ic-6. Therefore, the calcined material Ic-6 has been selected for our preliminary photocatalytic measurement. The peak intensity of Ic-6 increases with the addition of an oxidant (1,4-benzoquinone) under the irradiation of light ($\lambda > 460$ nm) but decreases with the addition of a reductant (pyrogallol) (Fig. 3), suggesting the formation of a cation radical on the carbon cluster. It is thus deduced that an electron transfer from carbon cluster to HfO_2 particle takes place to form an oxidation site at the carbon cluster and a reduction site at the HfO_2 particle.

The photo-catalytic activity of Ics was also examined. The reduction reaction of methylene blue in the presence of Ics was carried out. Fig. 4 shows the UV–vis spectra of methylene blue in the presence of Ic-6 under the irradiation of visible light ($\lambda > 460$ nm). The absorption band of methylene blue decreases with increase of the irradiation time. It should be indicated that there is no decomposition of methylene blue takes place in the dark. The results clearly demonstrate that the calcined materials have visible light-responsive catalytic activity. The catalytic activity (*ra*) of Ics was obtained by the equation *ra* = (the amount of decomposed methylene blue) × (g of the calcined material)$^{-1}$ × (h)$^{-1}$, and the results are also shown in Table 2. Here again, Ic-6 shows the highest *ra* value, indicating that Ic-6 have the highest photo-catalytic activity.

The surface of Ic-6 was loaded with CeO_2 particles, according to the procedure described in Section 2.4. The elemental analysis of Ic-6·CeO_2 shows the content of Ce is 1.14% in it. The Raman Spectrum of Ic-6·CeO_2 shows a frequency at 460 nm^{-1} due to Ce–O bond. SEM–EDX observation of Ic-6·CeO_2 shows that Ce atom is

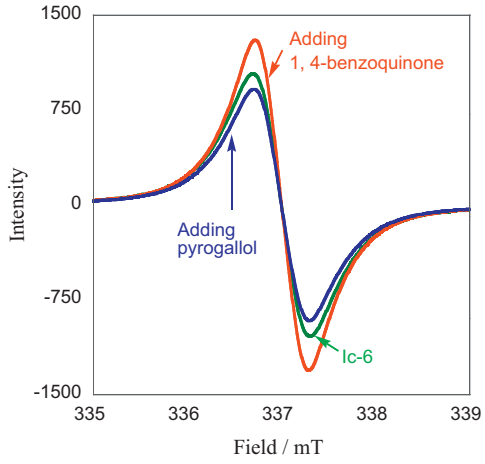

Fig. 3. ESR spectra of calcined material Ic-6 in the presence of 1,4-benzoquinone and pyrogallol.

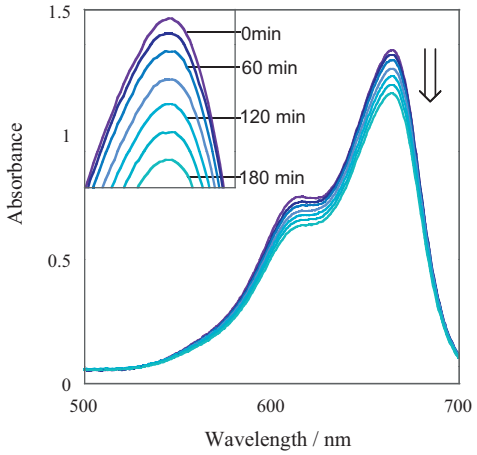

Fig. 4. UV–vis spectra of methylene blue in the presence of calcined material Ic-6 under the irradiation of light above 460 nm.

Table 3
Photo-decomposition of an aqueous $AgNO_3$ solution in the presence of Ic-6·CeO_2 and Ic-6rc.

Materials	μmol		Ratio $[O_2]$:[Ag]
	O_2	Ag	
Ic-6·CeO_2	0.85	3.57	1:4.2
Ic-6rc	0.51	2.33	1:4.5

uniformly dispersed on the surface of the matrix. The TEM observation (Fig. 5) of Ic-6·CeO_2 shows that particles with the diameters of ca. 1 nm, possibly CeO_2 particles, appeared on the interface of matrix, along with those of ca. 50 nm, possibly HfO_2 particles, in the carbon matrix. The oxidation–reduction reaction of an aqueous silver nitrate solution in the presence of Ic-6·CeO_2 and Ic-6rc was performed, where Ic-6rc was the material obtained by the re-calcination of Ic-6 at 300 °C for 3 h in an air atmosphere. As shown in Table 3, the O_2 and Ag produced from Ic-6·CeO_2 was higher than those from Ic-6rc, indicating that the CeO_2-loading on Ic-6 enhanced the photo-catalytic activity. If a four electron oxidation–reduction reaction takes place, the $[O_2]$:[Ag] ratio is given to be 1:4. The $[O_2]$:[Ag] ratio of Ic-6·CeO_2 was obtained to be 1:4.2, which is close to an ideal ratio. In other words, an effective charge-separation is considered to occur for Ic-6·CeO_2.

It is well known that the loading of noble metal atoms on the surface of semiconductors enhances their photo-catalytic activity. Thus, the surface of Ic-6·CeO_2 and Ic-6 are loaded with Pt particles to obtain Ic-6·CeO_2·Pt and Ic-6·Pt, respectively. The elemental analysis of the obtained materials shows the Pt contents of 0.75–0.77 wt%, and their TEM observation reveals the presence of particles with the diameters of ca. 1 nm, possibly Pt particles, in the matrix. Preliminary experiment on visible light-irradiated water decomposition reaction with Ic-6·CeO_2·Pt, Ic-6·CeO_2, Ic-6·Pt and Ic-6 was carried out according to the procedure described in Section 2.5 (Table 4). It is noted that the amount of H_2 and O_2

Table 4
Water decomposition in the presence of Ic-6·CeO_2·Pt, Ic-6·CeO_2, Ic-6·Pt and Ic-6 under the irradiation of light ($\lambda > 460$ nm).

Materials	nmol		Ratio $[H_2]/[O_2]$
	H_2	O_2	
Ic-6·CeO_2·Pt	117	526	0.22
Ic-6·CeO_2	78	430	0.18
Ic-6·Pt	110	0	–
Ic-6	0	0	–

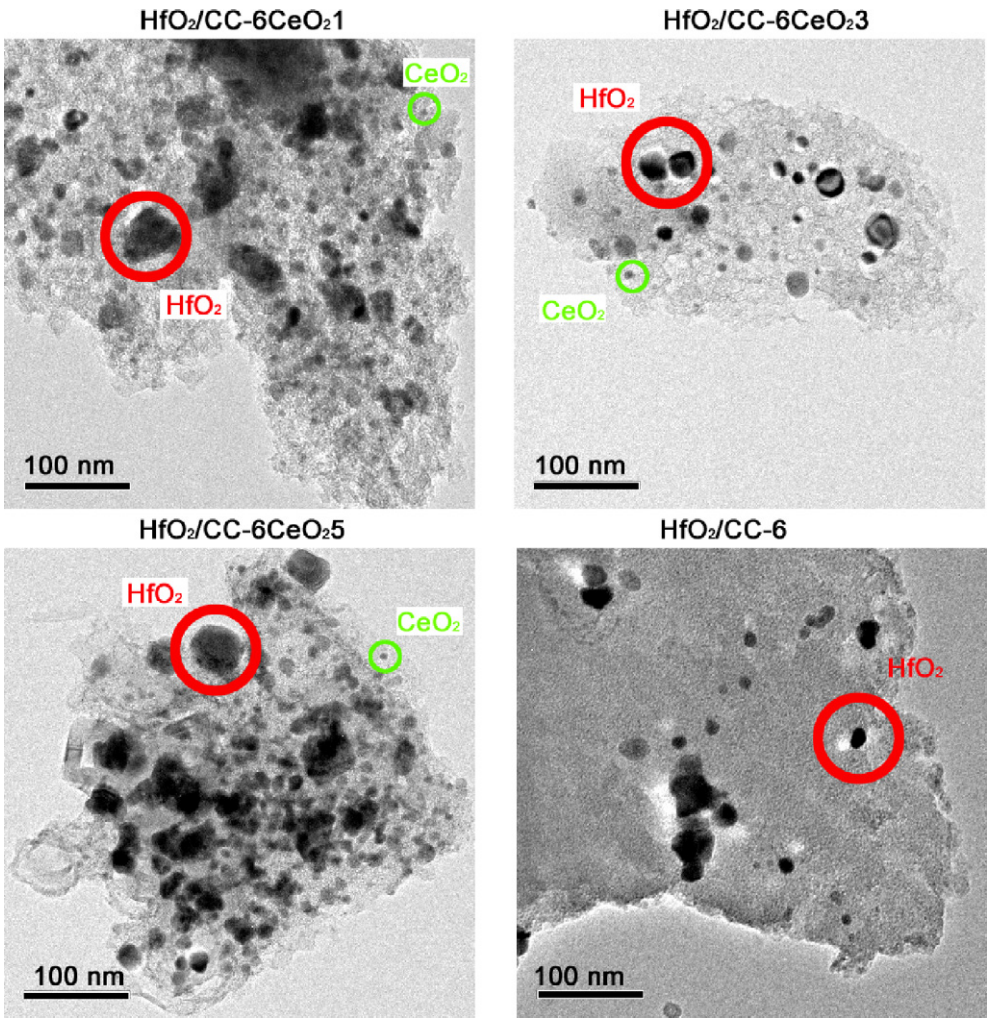

Fig. 5. TEM images of Ic-6·CeO_2.

evolved from Ic-6·CeO_2·Pt was higher than those from Ic-6·CeO_2, while no O_2 evolution was observed from Ic-6·Pt and no H_2 and O_2 evolution was detected from Ic-6, suggesting that the loading of the CeO_2 particles on Ic-6 enhanced the photo-catalytic activity. Here, if a four electron oxidation–reduction reaction of water takes place, then the $[H_2]/[O_2]$ of 2 will be given. However, it was found that the $[H_2]/[O_2]$ ratio observed for both Ic-6·CeO_2·Pt and Ic-6·CeO_2 were considerably smaller than 1, suggesting that an ideal four electron oxidation–reduction reaction did not takes place. We assume that the reason for this may be the loading of the CeO_2 on Ic-6 could decrease the reduction ability at the reduction site, since Ic-6·Pt was observed to evolve a considerable amount of H_2 without an O_2 generation. A possible assumption is that the CeO_2 particles were loaded not only on the oxidation site but also on the reduction site and the CeO_2 particles deposited at the reduction site may absorb electrons arrived from the oxidation site, thus decreases the reduction ability at the reduction site, although we could not offer any evidence at present. Therefore, in order to improve the photocatalytic ability of the material, a selective CeO_2-deposition on the oxidation site is considered to be necessary.

4. Conclusions

Nano-sized HfO_2/carbon cluster composite material was successfully prepared from $HfOCl_2$/starch complex by the microwave-irradiated calcination. The CeO_2 particles loaded-HfO_2/carbon cluster composite material was also successfully prepared. The synthesized CeO_2 particles loaded-HfO_2/carbon cluster composite material could decompose the aqueous silver nitrate solution and produce O_2 and Ag in the $[O_2]$:[Ag] ratio of 1:4.2. It confirms the good photocatalytic activity of the newly synthesized composite materials under visible light.

References

[1] M.A. Fox, Acc. Chem. Res. 32 (1999) 201.
[2] S. Karuppuchamy, J. Jeong, D.P. Amalnerkar, H. Minoura, Vacuum 80 (2006) 494.
[3] K. Sayama, K. Mukasa, R. Abe, Y. Abe, H. Arakawa, Chem. Commun. (2001) 2416.
[4] R. Konta, T. Ishii, H. Kato, A. Kudo, J. Phys. Chem. B 108 (2004) 8992.
[5] Y. Zhang, Z. Tang, X. Fu, Y.J. Xu, ACS Nano 12 (2010) 7303.
[6] S. Ge, H. Jia, H. Zhao, Z. Zheng, L. Zhang, J. Mater. Chem. 20 (2010) 3052.
[7] J. Zheng, Z. Liu, X. Liu, X. Yan, D. Li, W. Chu, J. Alloys Compd. 509 (2011) 3771.
[8] T. Oekermann, S. Karuppuchamy, T. Yoshida, D. Schelettwein, D. Woehrle, H. Minoura, J. Electrochem. Soc. 151 (2004) C62.
[9] N. Okada, S. Karuppuchamy, M. Kurihara, Chem. Lett. (2005) 16.
[10] X.B. Chen, S.H. Shen, L.J. Guo, S.S. Mao, Chem. Rev. 110 (2010) 6503.
[11] T. Kawahara, H. Miyazaki, S. Karuppuchamy, M. Ito, M. Yoshihara, Vacuum 81 (2007) 680.
[12] H. Matsui, S. Yamamoto, T. Sasai, S. Karuppuchamy, M. Yoshihara, Electrochemistry 75 (2007) 345.
[13] T. Furukawa, H. Matsui, H. Hasegawa, S. Karuppuchamy, M. Yoshihara, Solid State Commun. 142 (2007) 99.
[14] M. Jayalakshmi, K. Balasubramanian, Int. J. Electrochem. Sci. 4 (2009) 878.
[15] L.N. Dlaminia, R.W. Krausea, G.U. Kulkarnic, S.H. Durbach, Mater. Chem. Phys. 129 (2011) 406.
[16] J. Matos, J. Laine, J.-M. Herrmann, Appl. Catal. B: Environ. 18 (1998) 281.
[17] C.G. Silva, J.L. Faria, J. Photochem. Photobiol. A 155 (2003) 133.

[18] G. Colón, M.C. Hidalgo, M. Macías, J.A. Navío, J.M. Doña, Appl. Catal. B: Environ. 43 (2003) 163.
[19] N.M. Mahmoodia, M. Aramia, J. Zhang, J. Alloys Compd. 509 (2011) 4754.
[20] M. Krissanasaeranee, S. Wongkasemjit, A.K. Cheetham, D. Eder, Chem. Phys. Lett. 496 (2010) 133.
[21] F. D'Souza, O. Ito, Chem. Commun. 33 (2009) 4913.
[22] G. Jiang, Z. Lin, C. Chen, L. Zhu, Q. Chang, N. Wang, W. Wei, H. Tang, Carbon 49 (2011) 2693.
[23] T. Lv, L. Pan, X. Liu, T. Lu, G. Zhu, Z. Sun, J. Alloys Compd. 509 (2011) 10086.
[24] H. Yan, H. Yang, J. Alloys Compd. 509 (2011) L26.
[25] L. Li, W. Zhu, P. Zhang, Z. Chen, W. Han, Water Res. 37 (2003) 3646.
[26] S. Battiston, M. Bolzan, S. Fiameni, R. Gerbasi, M. Meneghetti, E. Miorin, Carbon 47 (2009) 1321.
[27] S. Battiston, M. Minella, R. Gerbasi, F. Visentin, P. Guerriero, A. Leto, Carbon 48 (2010) 2470.
[28] T. Kawahara, T. Kuroda, H. Matsui, M. Mishima, S. Karuppuchamy, Y. Seguchi, M. Yoshihara, J. Mater. Sci. 42 (2007) 3708.
[29] H. Matsui, S. Karuppuchamy, J. Yamaguchi, M. Yoshihara, J. Photochem. Photobiol. A: Chem. 189 (2007) 280.
[30] H. Miyazaki, H. Matsui, T. Nagano, S. Karuppuchamy, S. Ito, M. Yoshihara, Appl. Surf. Sci. 254 (2008) 7365.
[31] H. Matsui, K. Otsuki, H. Yamada, T. Kawahara, M. Yoshihara, J. Colloid Interface Sci. 297 (2006) 672.
[32] H. Matsui, T. Kawahara, R. Kudo, M. Uda, S. Karuppuchamy, M. Yoshihara, J. Alloys Compd. 462 (2008) L20.
[33] H. Matsui, T. Okajima, S. Karuppuchamy, M. Yoshihara, J. Alloys Compd. 468 (2009) L27.